JOURNAL OF CATALYSIS **158,** 561–569 (1996)
ARTICLE NO. 0054

Skeletal Isomerization of 1-Butene on MCM-22 Zeolite Catalyst

M. A. Asensi, A. Corma, and A. Martínez[1]

Instituto de Tecnología Química, UPV - CSIC, Universidad Politécnica de Valencia, Avda. de los Naranjos s/n, 46022 Valencia, Spain

Received April 12, 1995; revised September 20, 1995; accepted September 28, 1995

The skeletal isomerization of 1-butene has been studied on two MCM-22 zeolite catalysts synthesized with different Si/Al ratios, i.e., 15 and 47, under a wide range of operating conditions. Product yields are a function of *n*-butene conversion, and a maximum of isobutene yield is found at ca. 50% conversion. Besides isobutene, propylene and pentenes, which are formed by dimerization-cracking reactions, are the main products formed on MCM-22, while C_9 and heavier hydrocarbons are not observed in the reaction products. Isobutene also takes part, together with the *n*-butenes, in the formation of by-products through dimerization and/or codimerization processes, which would also lead to a lower isobutene selectivity. Moreover, the yield of isobutene increases with increasing reaction temperature and decreasing 1-butene partial pressure, while the contrary holds for the formation of by-products. On the basis of these results the mechanism of formation of isobutene and the different by-products on MCM-22 is discussed. Finally, the selectivity to isobutene is strongly improved by increasing the Si/Al ratio of the zeolite, which is explained by a decrease of the undesired consecutive reactions when decreasing the density of Brønsted acid sites of the zeolite.

1. INTRODUCTION

The addition of higher amounts of oxygenated compounds, such as methyl tert-butyl ether (MTBE), tert-amyl methyl ether (TAME), or ethyl tert-butyl ether (ETBE) to the gasoline pool is being adopted in many refineries worldwide (1) in order to reduce toxic emissions from vehicle exhausts, as well as to boost the octane of lead-free gasoline. As a consequence, the growing demand for isobutene, which is a raw material for the production of MTBE and ETBE, can not be satisfied by the FCC (fluid catalytic cracking) and steam cracking units which are the main isobutene sources in the actual refinery schemes. In this respect, skeletal isomerization of the much more abundant *n*-butenes appears to be a very attractive alternative for producing the required isobutene.

A number of solid acids have been studied as potential catalysts for the skeletal isomerization of linear butenes (2). Among them, halogenated aluminas and crystalline microporous materials (zeolites and zeotypes) were the most active and selective. In the case of zeolites and zeotypes, and owing to a high concentration of reactants inside the micropores and cavities, oligomerization of the *n*-butenes is a serious competing reaction that may decrease the selectivity to isobutene and can promote catalyst deactivation through hydrogen transfer and coking reactions. The extent of such undesired bimolecular processes can be decreased by decreasing the partial pressure of *n*-butenes in the feed and/or by using high reaction temperatures (2). However, higher temperatures can promote extensive cracking and limit the yield of isobutene due to thermodynamic considerations.

Furthermore, besides the above factors, there are other parameters that may affect the activity and selectivity of zeolites during the isomerization of *n*-butenes, i.e., the acidity of the catalyst and the geometrical restrictions imposed by the particular framework topology of these materials. In the first case, it has been reported that the presence of strong acid sites favor the undesired oligomerization-cracking reactions, whereas weak acid sites are more selective for isomerization (3). In this sense, boron-substituted zeolites (4–6) and aluminophosphates of the SAPO and MeAPO type (7, 8), having acid sites of weak-medium strength have been studied as isomerization catalysts, although they usually require temperatures above 500°C to be active and selective, with the corresponding detrimental effect on isobutene equilibrium yield. By contrast, zeolites (aluminosilicates) having strong acid sites are capable of performing the reaction at lower temperatures, but in this case the second factor, i.e., the pore structure of the zeolite, becomes a key parameter to achieve high yields and selectivities to isobutene. In this sense, medium pore 10MR zeolites were predicted to be more selective than large pore 12MR structures (9) by preventing extensive oligomerization inside their narrower pores. Furthermore, there appear to be large differences in product selectivity between 10MR zeolites depending on the particular topology of the zeolite structure. For instance, unidirectional 10MR zeolites, such as Theta-1, ZSM-22, and ZSM-23

[1] To whom correspondence should be addressed.

0021-9517/96 $12.00

are more selective than zeolite ZSM-5, the latter having a bidirectional system of intersecting 10MR channels (2). Moreover, ferrierite was found to be even more selective than the above zeolites, affording high yields of isobutene with high selectivity at relatively low temperatures (ca. 350°C) and without the need of using any diluent in the feed (10). This peculiar catalytic behavior of ferrierite has been related to its particular pore topology having interconnected 10MR and 8MR channels (11). However, whether or not this behavior is unique for ferrierite is still an open question that merits testing on new zeolite structures. In this way, the recently synthesized MCM-22 zeolite (12) has been shown to have a peculiar structure formed by two independent 10MR multidimensional system of channels, one of them sinusoidal and the other containing large supercages defined by 12MR of 7.1 Å inner diameter and 18.2 Å height (13), which gives it catalytic properties intermediate between 10MR and 12MR zeolites (14).

In this work we have investigated the catalytic performance of zeolite MCM-22 for the branching isomerization of 1-butene under a wide range of operating conditions, i.e., temperature, 1-butene space velocity, 1-butene partial pressure in the feed, and time on stream. Moreover, the influence of zeolite Si/Al ratio on activity and selectivity has also been studied. On the basis of these results the mechanism of formation of isobutene and by-products is also discussed.

2. EXPERIMENTAL

2.1. Synthesis and Characterization of Zeolite MCM-22

Two samples of zeolite MCM-22 with different Si/Al ratios were synthesized following the procedure described in Ref. (15) and using hexamethyleneimine (HM) as template. Gels of the molar composition 2.7 $Na_2O : Al_2O_3 : x\ SiO_2 : y$ HM : 1347 H_2O were prepared from NaOH (Prolabo), $NaAlO_2$ (Carlo Erba, 56% Al_2O_3, 37% Na_2O), SiO_2 (Aerosil 200, Degussa), and HM (Aldrich), where $x = 30$ and $y = 10.5$ for sample A, and $x = 100$ and $y = 50$ for sample B.

Crystallization of the gels was carried out in Teflon-lined stainless steel 60-ml autoclaves rotated at 60 rpm at temperatures of 150 and 135°C for samples A and B, respectively. After the autoclaves were cooled the product was filtered, washed with deionized water, and dried at 80°C overnight. Finally, the solids were calcined in air at 580°C for 3 h, exchanged with a 2 *M* NH_4Cl aqueous solution (80°C for 1 h), and calcined again at 500°C for 3 h in order to obtain the acid form of the zeolites.

The final catalysts were characterized by XRD (Phillips PW 1830, Cu$K\alpha$ radiation), IR spectroscopy with adsorbed pyridine (Nicolet FTIR 710), and scanning electron microscopy (SEM).

2.2. Catalytic Experiments

The isomerization of 1-butene (>99% pure) was performed at atmospheric pressure in a conventional continuous flow fixed-bed reactor having 10 mm inner diameter and 48 cm length. The zeolite powder was pressed, crushed, sieved to 0.59–0.84 mm particle size, and mixed with inert silica up to a constant bed volume of 2.3 cm^3 before being introduced into the reactor. The catalyst was activated at 400°C for 1 h under 270 cm^3/min of nitrogen before starting a reaction run. Then, a mixture of 1-butene and nitrogen (total flow rate above 300 cm^3/min to avoid external diffusion) is passed through the reactor (considered as time zero) at the desired reaction temperature, with the 1-butene and nitrogen flow rates adjusted to obtain the desired 1-butene partial pressure in the feed. The 1-butene space velocity, WHSV, was varied between 4.5 and 50 h^{-1} in order to obtain different conversion levels, either by changing the 1-butene flow rate or the amount of zeolite (typically between 0.05–1.00 g) in the catalyst bed.

The unconverted *n*-butenes and the reaction products were analyzed on line in a gas chromatograph (HP 5890 Series II) equipped with a KCl/Al_2O_3 column (50 m length, 0.32 mm internal diameter) and a flame ionization detector (FID), with the first analysis being done after 30 min on stream.

3. RESULTS AND DISCUSSION

3.1. Physicochemical Characteristics of MCM-22 Catalysts

The XRD patterns of the calcined samples A and B (Fig. 1) showed the presence of a pure crystalline MCM-22 phase according to the intensity and position of the diffraction peaks previously reported (16).

Table 1 shows the chemical composition, and the acidity of the two samples as measured by IR spectroscopy with adsorbed pyridine and desorbed at different temperatures. The amount of Brønsted and Lewis sites given in Table 1 was calculated from the intensity of the 1450 and 1550 cm^{-1} IR bands, respectively, and using the extinction coefficients given in Ref. (17). It is seen that MCM-22 sample A, synthesized with a lower Si/Al ratio, possesses a higher concentration of Brønsted acid sites than sample B, in agreement with a higher aluminum content in the former sample. Both samples show a relatively high proportion of strong Brønsted sites retaining pyridine after desorption at 400°C. The observed Lewis acidity can be related with extraframework Al species, indicating that some dealumination took place during the calcination steps. Thus, Table 1 indicates that the extent of dealumination was lower in the case of sample B synthesized with a higher Si/Al ratio.

Finally, the SEM micrographs of MCM-22 showed crystals having a hexagonal platelet morphology with an aver-

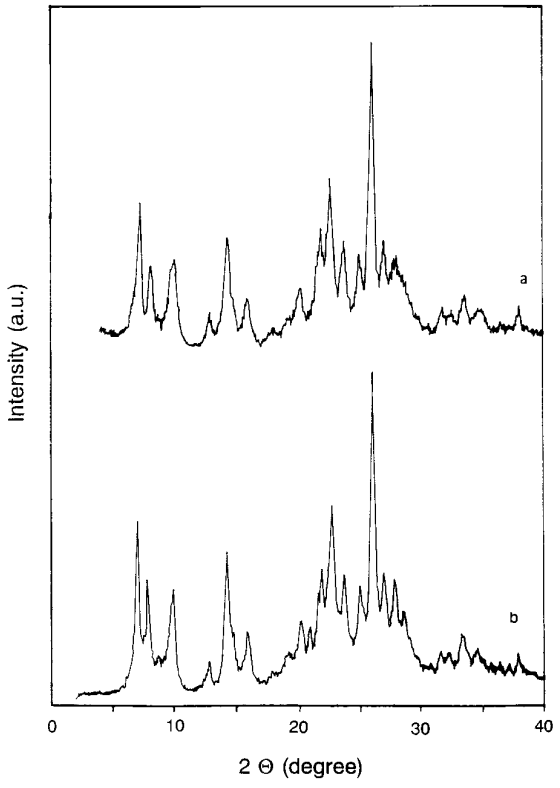

FIG. 1. X-ray diffraction patterns of calcined MCM-22: (a) sample A, (b) sample B.

age diameter of 0.3–0.5 μm. No large differences in morphology and size of the crystallites of samples A and B could be appreciated in the SEM micrographs.

3.2. Catalytic Isomerization of 1-Butene

Under the whole range of reaction conditions studied the 1-butene was seen to rapidly isomerize on the MCM-22 catalysts to the *cis*- and *trans*-2-butene isomers, giving a mixture of *n*-butenes in the product with a composition very close to the predicted thermodynamic equilibrium. Then, for simplicity we have grouped all the *n*-butenes to calculate conversion and product selectivities. Thus, conversion is defined here as the sum of the yields of all compounds other than *n*-butenes, while selectivity is given by the yield divided by the total *n*-butene conversion. Yields to the different reaction products are calculated according to the following equation:

$$\%\ \text{yield}\ (i) = \frac{\text{mole of product } i \text{ formed}}{\text{mole of 1-butene fed}} \times 100. \qquad [1]$$

The influence of time on stream (TOS), 1-butene space velocity, reaction temperature, and 1-butene partial pressure on the activity and selectivity of MCM-22 sample A will be discussed in the following sections. Then, the influence of zeolite Si/Al ratio will be studied by carrying out isomerization experiments on MCM-22 sample B.

A. Influence of time on stream (TOS). The evolution of *n*-butene conversion, isobutene yield and isobutene selectivity with TOS measured at 450°C, WHSV of 28 h^{-1}, and 0.1 atm of 1-butene in the feed are presented in Fig. 2. It can be seen there that conversion slightly decreases, while both isobutene yield and selectivity slightly increase during the period of 10 h on stream studied. The increase of isobutene yield and selectivity with TOS has also been observed during 1-butene isomerization on other 10MR zeolites, such as ZSM-22 (18) and ZSM-23 (19). This effect was explained considering that coking occurred first on the strongest acid sites responsible for the formation of by-products through oligomerization and cracking reactions, while the sites of lower acid strength still remained active for isomerization. Besides that, it was also suggested that

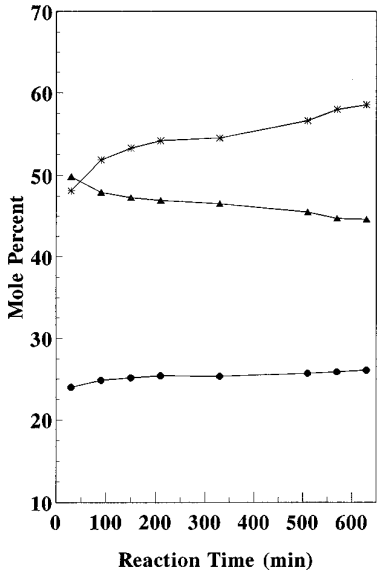

FIG. 2. n-Butene conversion (▲), isobutene yield (●), and isobutene selectivity (*) obtained on sample A at 450°C, 28 h^{-1} WHSV, and 0.1 atm 1-butene, as a function of time on stream (TOS).

TABLE 1

Physicochemical Properties of MCM-22 Catalysts

Sample	Chemical analysis		Acidity (μmol/g)					
			Brønsted			Lewis		
	Si/Al ratio	Na_2O (wt%)	250°C	350°C	400°C	250°C	350°C	400°C
A	15.2	0.026	75	49	28	37	27	23
B	46.8	0.001	28	17	6	12	10	6

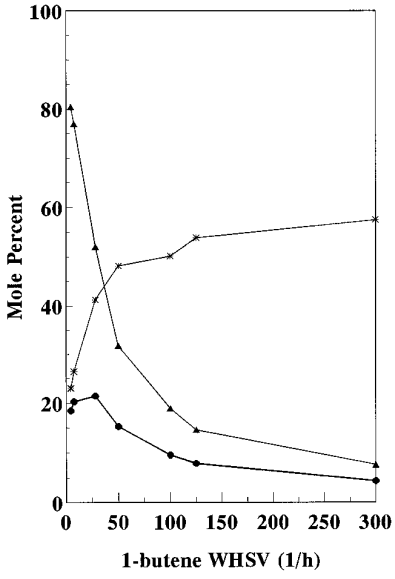

FIG. 3. Influence of 1-butene space velocity on conversion (▲), isobutene yield (●), and isobutene selectivity (*) on MCM-22 sample A. Reaction conditions: 350°C, 0.1 atm 1-butene, and 30 min TOS.

coke deposits could reduce the free space around the acid sites thus decreasing the effective pore size of the zeolite and favoring isomerization against the more steric demanding oligomerization. Moreover, poisoning of external surface acid sites, which would be more selective for oligomerization, may also contribute to the increased isobutene selectivity as the catalyst ages. These effects could also explain why "fresh" ferrierite produces initially a very high concentration of by-products, and only when the amount of coke deposited on the zeolite reaches a certain level does it become very selective for producing isobutene (11). However, in the case of MCM-22 sample A with a relatively high Al content and having a high proportion of very strong acid sites, there is another factor that may explain the increase of isobutene yield with TOS, and this is the decrease of acid site density as the zeolite becomes poisoned. Decreasing the acid site density would decrease the extent of secondary consecutive reactions, such as oligomerization, while favoring isomerization. This will be further discussed when studying the influence of zeolite Si/Al ratio during 1-butene isomerization.

B. Influence of 1-butene space velocity (WHSV). The effect of 1-butene WHSV on conversion, isobutene yield, and selectivity at 350°C and 0.1 atm of 1-butene in the feed is shown in Fig. 3. Unless otherwise specified, and owing to the low deactivation rate observed for the MCM-22 catalysts, the catalytic data given in this work will correspond to the values obtained after 30 min TOS. Under these conditions conversion decreases and isobutene selectivity increases with increasing WHSV, whereas the yield of isobutene first increases rapidly, goes through a maximum at ca. 30 h^{-1}, and then decreases at higher WHSV. Thus, low space velocities (high contact times) produce low isobutene selectivities by favoring undesired secondary reactions, such as oligomerization, cracking, and hydrogen transfer leading to by-product formation. Besides isobutene, C_2 to C_8 unsaturated and saturated hydrocarbons were also formed during the reaction. Among these, propylene and pentenes were the major by-products formed on the MCM-22 catalyst.

In order to obtain information on the different reactions occurring during the isomerization of *n*-butenes on zeolite MCM-22 the product yields have been presented as a function of conversion in Fig. 4. It can be seen that isobutene, C_3, C_5, and saturated butanes (*n*-butane and isobutane) are all formed at low conversions and can be considered as primary products (Fig. 4a). The proportion of propane and pentanes in the C_3 and C_5 fragments is initially very low, and increases with conversion as it occurs with the butanes. On the other hand, C_2 and C_6–C_8 hydrocarbons are secondary products as they are formed at higher conversions (Fig. 4b). No hydrocarbons higher than C_8 are observed in the reaction products in the whole range of conversions studied.

Figure 4a shows that the yield of isobutene first increases, passes a maximum at ca. 50% conversion, and then declines at higher conversion levels. Above 70% conversion the concentration of isobutene in the products becomes determined by the thermodynamic equilibrium between the butenes (dashed line in Fig. 4a), and dimerization (oligomerization)-cracking become the predominant reactions. It is also seen in Fig. 4a that the C_3/C_5 ratio is very close to unity at low conversions, indicating that C_3 and C_5 are initially formed from a common intermediate, i.e., C_8 dimers which are rapidly cracked by β-scission on the strong acid sites of MCM-22. However, the C_3/C_5 ratio increases at higher conversions, suggesting that some of the C_3 is also formed by cracking of hydrocarbons other than C_8. At very high conversions (above 80%) the rate of formation of C_3 and C_5 decreases (Fig. 4a), while that of C_6 and C_7 hydrocarbons strongly increases (Fig. 4b).

The formation of C_6 and C_7 may be explained considering the cracking of C_{12} or even larger oligomers as

$$i\text{—}C_8^+ + C_4 = \rightleftharpoons [i\text{—}C_{12}]^+$$

$$\xrightarrow[-H^+]{\beta\text{-scission}} \begin{cases} 2\,i\text{—}C_6= & [2] \\ i\text{—}C_5= + i\text{—}C_7= & [3] \end{cases}$$

while further recracking of the C_6 and C_7 formed could account for the increase of the C_3/C_5 ratio as conversion increases.

Recently (19), recombination of C_3 and C_4 fragments has been considered in order to explain the formation of hexenes and heptenes during the isomerization of *n*-bu-

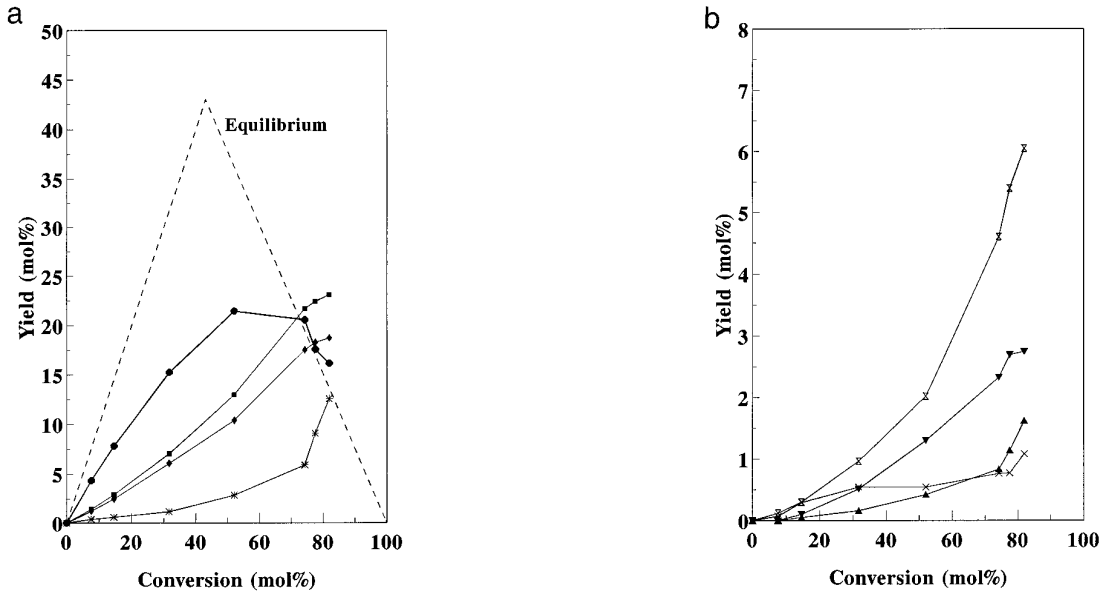

FIG. 4. Product yields obtained on sample A as a function of n-butene conversion. (a) Primary products: C_3 (■), n-butane + isobutane (*), isobutene (●), C_5 (◆). The dashed line represents the isobutene equilibrium yield. (b) Secondary products: C_2 (▲), C_6 (▽), C_7 (▼), C_8 (X). Reaction conditions are as in Fig. 3.

tenes on ZSM-23 zeolite. This zeolite has unidimensional 10MR channels of 4.5×5.2 Å diameter (20), and therefore, formation of branched C_{12} or larger oligomers inside its channels should be strongly hindered. In the case of MCM-22, oligomerization may well take place in the large 12MR cavities, although it should be more impeded in the tortuous 10MR system of MCM-22. However, even if the oligomers can be formed in the large cages, they should diffuse out through 10MR windows, thus favoring their cracking into lighter fragments. This could also explain the absence of C_9 and higher hydrocarbons and the relatively low concentration of octenes in the reaction products. Nevertheless, dimerization and/or codimerization of C_3–C_5 cannot be ruled out in order to explain the distribution of by-products at very high conversions.

The complex product distribution observed during 1-butene isomerization clearly shows the difficulty in establishing a simple reaction mechanism, since, besides the skeletal isomerization, a large number of consecutive and parallel reactions also take place. Indeed, there are controversial opinions in the literature concerning the mechanism of formation of isobutene and by-products. In the latter case, some authors claimed that by-products are formed exclusively from the *n*-butenes (4), while others stated that both *n*-butenes and isobutene can lead to the formation of by-products (19). The latter assumption was based on the observation that a similar product distribution was obtained when feeding *n*-butenes or isobutene on zeolite ZSM-23 under the same experimental conditions.

In our case we have carried out isomerization experiments on the MCM-22 catalyst, feeding pure 1-butene, pure isobutene, and 1-butene/isobutene mixtures under identical reaction conditions, i.e., 0.1 atm partial pressure of olefin, 350°C reaction temperature, and WHVS of 28 h^{-1} based on total butene fed. The molar composition of the reaction products obtained after 30 min TOS is given in Table 2. Several general conclusions can be derived from these experiments. First, a very close product distribution, with the obvious exception of *n*-butenes and isobutene, is obtained when feeding either 1-butene or isobutene, in agreement with the results reported in Ref. (19) on a ZSM-23 zeolite. Furthermore, we also observed a similar distribution of by-products when feeding the 1-butene/isobutene mixtures. These results may indicate that both *n*-butenes and isobutene participate in the formation of by-

TABLE 2

Product Distribution Obtained on MCM-22 Sample A when Feeding 1-Butene, Isobutene, and 1-butene/Isobutene Mixtures at 350°C, 0.1 atm of Olefin, 28 h^{-1} WHSV, and 30 Min TOS

Composition of the olefin feed (%)		Product distribution (mol%)						
1-Butene	Isobutene	C_2	C_3	C_4°	$nC_4^=$	$iC_4^=$	C_5	C_{6+}
100	0	0.22	10.20	2.12	57.39	17.93	8.80	3.34
83	17	0.18	9.39	1.74	53.32	23.60	8.61	3.16
67	33	0.18	9.76	1.82	47.81	28.55	8.77	3.10
0	100	0.17	8.74	1.67	18.41	57.11	8.42	5.49

TABLE 3

Influence of Reaction Temperature on Conversion and Product Yields[a]

T (°C)	Conversion (mol%)	Yield (mol%)[b]						% $i-C_4^=$ with respect to equilibrium
		C_2	C_3	C_4°	i-$C_4^=$	C_5	C_{6+}	
250	11.9	0.0	1.1	0.6	4.4	2.2	3.6	10
300	22.9	0.1	2.9	1.1	9.2	4.2	5.4	23
350	52.3	0.4	13.0	2.9	21.5	10.4	4.2	71
400	51.7	0.6	12.8	1.9	25.7	8.4	2.3	85
450	55.1	1.5	15.1	2.3	26.5	7.9	1.7	95
500	49.8	2.1	11.2	1.3	29.6	5.2	0.5	100

[a] Reaction conditions: WHSV = 28 h^{-1}, 0.1 atm of 1-butene, TOS = 30 min.
[b] C_4° = isobutane + n-butane. The other fractions include both saturated and unsaturated hydrocarbons.

products, and that the dimerization-cracking process, the main secondary reaction leading to propylene and pentenes, is very similar whether the C_8 intermediates are formed from dimerization of n-butenes, codimerization of n-butenes with isobutene, or dimerization of isobutene.

$$n\text{—}C_4{=} + n\text{—}C_4{=} \longrightarrow [i\text{—}C_8{=}] \xrightarrow{\text{cracking}} C_3{=} + C_5{=} \quad [4]\text{–}[6]$$

$$n\text{—}C_4{=} + i\text{—}C_4{=} \longrightarrow [i\text{—}C_8{=}] \xrightarrow{\text{cracking}} C_3{=} + C_5{=} \quad [4]\text{–}[6]$$

$$i\text{—}C_4{=} + i\text{—}C_4{=} \longrightarrow [i\text{—}C_8{=}] \xrightarrow{\text{cracking}} C_3{=} + C_5{=} \quad [4]\text{–}[6]$$

Moreover, by comparing the results obtained when feeding pure 1-butene and pure isobutene it can be concluded that the skeletal isomerization of n-butenes is a reversible process with both isomerization of n-butenes to isobutene and that of isobutene to n-butenes occurring at similar reaction rates.

Reactions [5] and [6], in which isobutene participate, would be increasingly important as the concentration of isobutene in the reaction products increases, and would explain the decrease in isobutene yield observed in Fig. 4a in the 50–70% conversion range, before the isobutene yield starts to be limited by the thermodynamic equilibrium.

C. Influence of reaction temperature. The effect of temperature on conversion and product yields is shown in Table 3 at 28 h^{-1} WHSV and 0.1 atm partial pressure. Under these conditions the n-butene conversion rapidly increases up to 350°C and then remains practically constant at higher temperatures. The yield of isobutene continuously increases and reaches the predicted equilibrium yield at ca. 500°C. On the other hand, the total amount of by-products first increases, passes a maximum at ca. 350°C and then decreases upon further increase of reaction temperature. At temperatures below 350°C C_6–C_8 hydrocarbons are the major by-products, while propylene and pentenes are the predominant by-products in the 350–500°C range, owing to a higher extent of cracking reactions at high temperatures.

The decrease of the total yield of by-products above 350°C probably occurs because the dimerization of the butenes becomes thermodynamically unfavored at high reaction temperatures. The different behavior observed for isobutene strongly suggests that this product and the by-products are really formed on MCM-22 through different mechanisms. Usually, it is assumed that isobutene is produced from n-butenes by a monomolecular mechanism involving the formation of a very unstable primary carbocation.

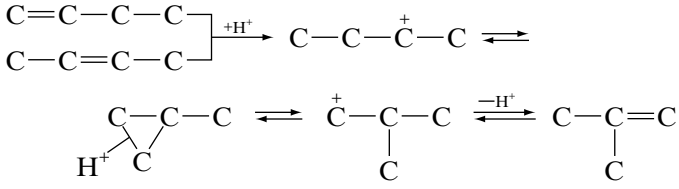

However, in some cases it has also been suggested that isobutene can be formed by a bimolecular mechanism involving the dimerization of n-butenes, rearrangement of the C_8 intermediate, and further cracking.

$$2\,n\text{—}C_4{=} \rightleftharpoons [i\text{—}C_8{=}] \longrightarrow 2\,i\text{—}C_4{=} \quad [7]$$

Indeed, this mechanism has been proposed to occur on the ferrierite zeolite in order to explain the high selectivity of this catalyst (11), and also on modified aluminas where in some cases isobutene concentrations above the thermodynamic equilibrium were observed (21, 22).

In the case of MCM-22 catalyst the results of Table 3 allow us to advance that, although reaction [7] cannot be completely excluded, this is not the main mechanism producing isobutene, since otherwise the yield of isobutene and by-products, which are really formed through a dimerization-cracking pathway, should follow the same trends with reaction temperature. Further support to this will be

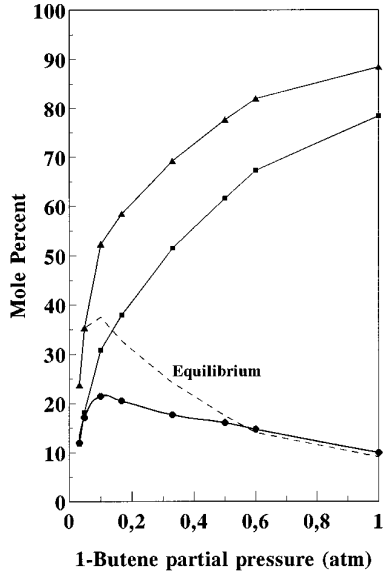

FIG. 5. Influence of 1-butene partial pressure for MCM-22 sample A on conversion (▲), isobutene yield (●), and total by-products yield (■). The dashed line represents the isobutene equilibrium yield. Reaction conditions: 350°C, 28 h^{-1} WHSV, and 30 min TOS.

given in the following section which discusses the effect of 1-butene partial pressure.

D. Influence of 1-butene partial pressure. The partial pressure of 1-butene in the feed is expected to have a larger influence on bimolecular than on unimolecular processes. Figure 5 shows the yield to isobutene and total by-products as a function of 1-butene partial pressure at 350°C and 28 h^{-1} WHSV. It is clearly seen that isobutene and by-products follow different trends when increasing the olefin partial pressure. The yield of isobutene first increases, goes through a maximum at ca. 0.1 atm, and then continuously decreases with the 1-butene partial pressure. Above ca. 0.5 atm the isobutene yield practically follows the predicted equilibrium yield (dashed line in Fig. 5). On the contrary, the yield of by-products strongly increases when increasing the 1-butene partial pressure as a consequence of the increase of bimolecular processes, such as dimerization-oligomerization of the butenes. The decrease of isobutene yield observed above 0.1 atm may be attributed to the increase of dimerization and codimerization processes (reactions [5] and [6]), and also to the limited equilibrium yield of isobutene at high *n*-butene conversions.

Since the *n*-butene conversion increases with 1-butene partial pressure (Fig. 5), and product yields are a function of conversion (Fig. 4), the effect of partial pressure can be better seen when comparing the product selectivities at constant conversion and different 1-butene pressures (Table 4). It is clearly seen that isobutene selectivity continuously decreases with 1-butene partial pressure, while the opposite is observed for the by-products. Moreover, the selectivity to propylene and pentenes remains almost constant whereas that of C_6–C_8 compounds increases with partial pressure. These results indicate a strong increase of the bimolecular dimerization-oligomerization processes with increasing 1-butene partial pressure, and strongly suggest that isobutene is mainly formed on MCM-22 through a monomolecular mechanism, and not via dimerization-cracking as is the case of propylene and pentenes.

TABLE 4

Effect of 1-Butene Partial Pressure on Product Selectivities at ca. 50% Conversion at 350°C Reaction Temperature and 30 Min TOS

1-Butene partial pressure (atm)	Selectivities (mol%)				
	$C_2^=$	$C_3^=$	*i*-$C_4^=$	$C_5^=$	C_{6+}
0.1	0.8	24.4	41.0	18.8	8.0
0.5	0.7	22.2	31.7	18.9	19.4
1.0	0.9	21.7	26.6	18.7	23.7

E. Influence of the Si/Al ratio of MCM-22 zeolite. Figure 6 compares the product yields obtained on the MCM-22 samples A (Si/Al = 15) and B (Si/Al = 47) at 350°C, 0.1 atm of 1-butene, and WHSV of 28 h^{-1}. The rates of formation of the different reaction products on the two MCM-22 samples under the above reaction conditions are also given in Table 5. It can be seen in Fig. 6 that the isobutene yield remains practically constant while that of by-products strongly decreases with an increasing Si/Al ratio of the zeolite. According to the IR-pyridine data

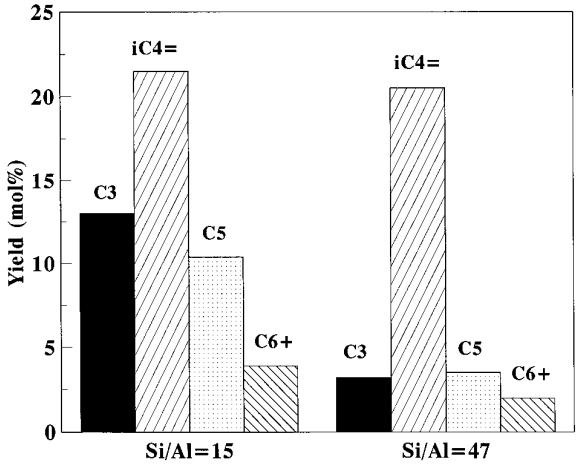

FIG. 6. Influence of the Si/Al ratio of MCM-22 zeolite on product yields obtained at 350°C, 0.1 atm 1-butene, 28 h^{-1} WHSV, and 30 min TOS.

TABLE 5

Rates of Formation (mmol/h g_{cat}) of the Different Reaction Products on MCM-22 Samples A (Si/Al = 15) and B (Si/Al = 47) at 350°C, 0.1 atm of 1-Butene, 28 h^- WHSV, and 30 Min TOS

Product	Sample A	Sample B
Methane	0.0	0.0
Ethane	0.0	0.0
Ethylene	2.1	0.2
Propane	1.0	0.1
Propylene	64.2	16.1
iso-Butane	10.7	1.6
n-Butane	3.6	1.4
iso-Butene	107.8	102.8
iso-Pentane	2.7	0.1
n-Pentane	0.3	0.1
Pentenes	49.3	17.8
C_{6+}	19.4	11.1

already shown in Table 1 there are not big differences in the acid strength distributions of the Brønsted sites in the two samples, but sample B has a much lower acid site density owing to its lower Al content. This indicates that, besides the possible influence of acid strength distribution, in the case of zeolites with strong Brønsted acid sites, such as MCM-22, the acid site density, which in turn depends on the framework Si/Al ratio of the zeolite, is a key parameter to control the selectivity to isobutene. This is explained by a decrease of the extent of consecutive reactions leading to by-products as the acid sites become more and more isolated. On top of that, the decrease of adsorption properties of the zeolite upon increasing the framework Si/Al ratio (23), which will decrease the concentration of olefins inside the zeolite pores thus decreasing the extent of bimolecular processes, may also be considered in order to explain the higher isobutene selectivity obtained on the MCM-22 sample with higher Si/Al ratio.

The fact that the isobutene yield remains at the same level while that of by-products is considerably reduced upon increasing the zeolite Si/Al ratio suggests again that isobutene should be mainly formed on MCM-22 via direct isomerization of *n*-butenes, since monomolecular processes would be much less affected than bimolecular ones when changing the acid site density in the zeolite.

Furthermore, Table 6 shows the effect of reaction conditions on *n*-butene conversion and product yields for the high Si/Al ratio sample B. The same general trends that were already discussed for sample A can be applied for sample B. Increasing the reaction temperature increases both the yield and selectivity to isobutene, while increasing the 1-butene partial pressure favors undesired dimerization-oligomerization reactions thus decreasing the yield and selectivity to isobutene. Then, at nearly optimum operating conditions, a selectivity to isobutene of ca. 80% at ca. 40% conversion is obtained on MCM-22 sample B.

4. CONCLUSIONS

Zeolite MCM-22 has been shown to be an active and stable catalyst for the skeletal isomerization of 1-butene. The activity and selectivity were seen to depend on the reaction conditions, i.e., temperature, 1-butene partial pressure, and olefin space velocity. A maximum of isobutene yield was observed at ca. 50% *n*-butene conversion. At low conversions, isobutene, propylene, and pentenes, the latter two compounds formed by dimerization of the butenes followed by cracking, are the primary products obtained on MCM-22. In addition, some *n*-butane and isobutane are also initially formed through hydrogen transfer reactions. At high conversions the concentration of C_6 and C_7 compounds strongly increases while that of isobutene decreases due to the increase of secondary consecutive reactions and to the limited equilibrium yield of isobutene

TABLE 6

Influence of Reaction Conditions on Conversion and Product Yields Obtained at 30 min TOS During the Isomerization of 1-Butene on the MCM-22 Sample B (Si/Al = 47)

Reaction Conditions				Yield (mol%)					
T (°C)	P_p (1 − $C_4^=$) (atm)	WHSV (h^{-1})	Conversion (mol%)	C_2	C_3	C_4°	$i-C_4^=$	C_5	C_{6+}
350	0.1	14	46.3	0.1	6.2	1.0	29.4	6.4	3.2
350	0.1	28	30.1	0.1	3.2	0.6	26.1	4.1	0.9
400	0.1	28	36.3	0.1	4.5	0.6	26.1	4.1	0.9
450	0.1	28	36.3	0.2	3.5	0.5	28.4	3.1	0.6
350	0.5	28	60.3	0.3	9.5	3.3	22.2	11.6	13.4
350	1.0	28	76.8	0.5	10.7	7.3	15.8	16.7	25.8

in the product stream. Formation of C_6 and C_7 probably occurred by cracking of C_{12} or even larger oligomers that could be formed in the 12MR large cavities present in MCM-22. However, the concentration of C_8 was relatively low in the whole range of conversions, and no C_9 and higher hydrocarbons were observed in the reaction products. This was ascribed to the high cracking activity of the strong acid sites of MCM-22 (24), and also to a strong limitation for the large oligomers to diffuse out of the 12MR cages through the 10MR windows.

Experiments feeding isobutene and 1-butene/isobutene mixtures demonstrated that the skeletal isomerization is a reversible process, and that isobutene also intervenes in the formation of by-products, probably by dimerization and codimerization reactions, leading to a distribution of by-products closely resembling that obtained when feeding pure 1-butene.

The yield of isobutene increased with increasing reaction temperature and decreasing 1-butene partial pressure, while the opposite behavior was observed for the formation of by-products. These results strongly suggested different reaction mechanisms operating for both isobutene and by-product formation. The latter are formed through dimerization, oligomerization, and cracking reactions, while isobutene may be mainly formed on MCM-22 via direct isomerization of *n*-butenes through a monomolecular mechanism.

Finally, the selectivity to isobutene was strongly improved when the Si/Al ratio of the zeolite increased from 15 to 47. This was ascribed to a reduction of the bimolecular consecutive reactions with decreasing acid site density of the zeolite. Thus, a selectivity to isobutene of ca. 80% at ca. 40% conversion was obtained on the high Si/Al ratio MCM-22 sample at near optimum operating conditions.

ACKNOWLEDGMENT

Financial support by the Comisión Interministerial de Ciencia y Tecnología of Spain (Project MAT 94-0166) is gratefully acknowledged.

REFERENCES

1. Maxwell, I. E., and Naber, J. E., *Catal. Lett.* **12,** 105 (1992).
2. Butler, A. C., and Nicolaides, C. P., *Catal. Today* **18,** 443 (1993).
3. Choudary, V. R., *Chem. Ind. Dev.* **8,** 32 (1974).
4. Bianchi, D., Simon, M. W., Nam, S. S., Xu, W.-Q. Suib, S. L., and O'Young, Ch. L., *J. Catal.* **145,** 551 (1994).
5. Simon, M. W., Xu, W.-Q., Suib, S. L., and O'Young, Ch. L., *Microporous Mater.* **2,** 477 (1994).
6. O'Young, Ch. L., Xu, W.-Q., Simon, M. W., and Suib, S. L., "Studies in Surface Science and Catalysis," Vol. 84, p. 1671. Elsevier, Amsterdam, 1994.
7. Zubowa, H. L., Richter, M., Roost, V., Parlitz, B., and Fricke, R., *Catal. Lett.* **19,** 67 (1993).
8. Yang, S. M., Guo, D. H., Lin, J. S., and Wang, G. T., "Studies in Surface Science and Catalysis," Vol. 84, p. 1677. Elsevier, Amsterdam, 1994.
9. Thomas, J. M., *Sci. Am.* April, 112 (1992).
10. Grandvallet, P., de Jong, K. P., Mooiweer, H. H., Kortebeek, A. G. T. G., and Kraushaar-Czarnetzki, B., European Patent 501.577 (1992).
11. Mooiweer, H. H., de Jong, K. P., Kraushaar-Czarnetzki, B., Stork, W. H. J., and Krutzen, B. C. H., "Studies in Surface Science and Catalysis," Vol. 84, p. 2327. Elsevier, Amsterdam, 1994.
12. Rubin, M. K., and Chu, P., U.S. Patent 4,954,325 (1990).
13. Leonowicz, M. E., Lawton, J. A., Lawton, S. L., and Rubin, M. K., *Science* **264,** 1910 (1994).
14. Corma, A., Corell, C., Llopis, F., Martínez, A., and Pérez-Pariente, J., *Appl. Catal. A* **115,** 121 (1994).
15. Corma, A., Corell, C., and Pérez-Pariente, J., *Zeolites* **15,** 2 (1995).
16. Abril, R. P. L., Bowes, E., Green, G. J., Marler, D. O., Shihabi, D. S., and Socha, R. F., U.S. Patent 5,085,762 (1992).
17. Hughes, T. R., and White, H. M., *J. Phys. Chem.* **71,** 2192 (1967).
18. Simon, M. W., Suib, S. L., and O'Young, Ch. L., *J. Catal.* **147,** 484 (1994).
19. Xu, W.-Q., Suib, S. L., and O'Young, Ch. L., *J. Catal.* **150,** 34 (1994).
20. Wright, P. A., Thomas, J. M., Millward, G. R., Ramdas, S., and Barri, S. A., *J. Chem. Soc. Chem. Commun.,* 1117 (1985).
21. Cheng, Z. X., and Ponec, V., *Appl. Catal. A* **118,** 127 (1994).
22. Cheng, Z. X., and Ponec, V., *J. Catal.* **148,** 607 (1994).
23. Corma, A., Faraldos, M., Martínez, A., and Mifsud, A., *J. Catal.* **122,** 230 (1990).
24. Corma, A., Martínez-Alfaro, V., and Orchillés, A. V., *Appl. Catal.,* in press.